

# Ab-initio analysis of superstructures revealed by STM on bilayer graphene

E. Cisternas<sup>1</sup> and J. D. Correa<sup>2</sup>

<sup>1</sup>Departamento de Ciencias Físicas, Universidad de La Frontera, Casilla 54 D, Temuco, Chile

<sup>2</sup>Departamento de Ciencias Físicas, Universidad Andres Bello, Av. República 220, 837-0134 Santiago, Chile

E-mail: [ecisternas@ufro.cl](mailto:ecisternas@ufro.cl), [jcorrea@unab.cl](mailto:jcorrea@unab.cl)

**Abstract.** In this work we performed density functional theory calculations for a twisted bilayer graphene (BLG). Several commensurable rotation angles were analyzed and for each one a constant height mode STM image was obtained. These STM images, calculated under the Tersoff-Hamman theory, reproduce the main features experimentally observed, particularly superstructures and giant corrugations. In this way we confirm that STM characterization of twisted BLG can produce superstructures whose tunneling current intensity maxima occur over regions with AA stacking. Additionally we give new evidence in favour of an electronic origin for the superstructures instead another physical grounds.

## 1. Introduction

The increasing interest for nanoscience and nanotechnology has evidenced the importance of the scanning tunneling microscope (STM) to explore the nature at atomic scale. In this context graphene, a novel layered material with potential technological applications [1], has been intensively characterized by STM techniques and has revealed its surprising behavior: edge states at the border [2, 3], superstructures [4, 5, 6] and Van Hove Singularities [7]. The graphene particularities were implied before by STM characterization of the (0001) surface of highly oriented pyrolytic graphite (HOPG): difficulties to obtain STM complete atomic resolution as well the observation of superstructures are examples of this.

Extending the preceding statements, let us precise that graphene is a stable bidimensional structure formed by carbon atoms ordered in a hexagonal lattice (the first neighbor distance is 1.42 Å). In crystalline graphite (HOPG) such layers are stacked on each other in a  $AB$  sequence, and therefore it is possible to identify two type of atomic sites: the  $\alpha$ -type sites, corresponding to atoms with neighbors directly above and below in adjacent layers; and the  $\beta$ -type sites, which do not have direct neighbors in the adjacent layers. An important consequence of the crystalline structure of HOPG is that near the Fermi level the bulk presents a Local Density of States (LDOS) which is larger for atoms on  $\beta$ -type sites [8]. The theory of STM image formation [9, 10] considers that the accessible states by STM are those in the energy window  $[E_{Fermi} - eV_{bias}, E_{Fermi}]$ . Consequently in HOPG only those atoms on  $\beta$ -type sites appears visible for a STM operating at low bias voltages and they form the triangular lattice usually reported on experiments. However the LDOS of  $\alpha$  and  $\beta$  sites tends to be equal by increasing the bias voltages and the persistence of the triangular lattice at higher bias voltages has been explained by resolution losses introduced for the STM tip size [11].

Following the preceding ideas, the observation of superstructures during STM experiments can be explained by considering a relative rotation among the constituent graphene layers. This is because rotations generate *Moiré Patterns* where it is possible to identify regions with a high concentration of  $\beta$ -type sites, called  $g - \beta$  sites, and regions with a high concentration of  $\alpha$ -type sites, called  $g - \alpha$  or  $AA$  stacked regions [see Figure 1(a)]. In both cases  $g$  stands for *giant* [12]. In this frame the  $g - \beta$  regions would appear brilliant in STM images due to the large LDOS of atoms on  $\beta$  sites [12]. However, Rong and Kuiper [13], on base of first principles DOS calculations [14], proposed that brilliant zones occur over the  $g - \alpha$  regions. Additionally a third explanation for the superstructures considers that more important than the electronic effects induced by rotation between weakly interactive graphene layers, could be surface deformations introduced by STM tip while it scans the surface (see Ref. [15] and references therein). This has been a long standing controversy which has attracted renewed interest over the STM image formation of graphite surface [11, 16, 17, 18] and over the physical origin of superstructures [15, 19, 20, 21].

In this context, an important tool to analyze the effect of rotation among

graphene layers is the calculation of STM images and the corresponding contrast with experimental data. Following this objective we have focused in the task of generate STM images for different rotation angles between two graphene layers. We have organized this paper as follows: details of the images calculation are given in next section; theoretical results are summarized in section 3 and finally the main conclusions are presented.

## 2. Calculation Method

The system under study corresponds to BLG presenting a relative rotation angle between its layers (twisted bilayer graphene). Such rotation occurs around the stacking direction and despite for any angle one can identify a superstructure (or moiré pattern) only for very particular angles the misoriented layers are in commensuration [21, 22, 23]. A commensurable unit supercell requires a rotation from a vector  $\vec{V}_1 = m\vec{a}_1 + n\vec{a}_2$  to  $\vec{V}_2 = n\vec{a}_1 + m\vec{a}_2$ , where  $\vec{a}_1 = (\sqrt{3}, -1)a_0/2$  and  $\vec{a}_2 = (\sqrt{3}, 1)a_0/2$  are the graphene basis vectors;  $m$  and  $n$  are integers and  $a_0 = 2.46$  Å is the lattice constant. The commensurable rotation angle is defined by

$$\cos \theta = \frac{m^2 + 4mn + n^2}{2(m^2 + mn + n^2)}, \quad (1)$$

and the unit super cell vectors correspond to:  $\vec{t}_1 = \vec{V}_2 = n\vec{a}_1 + m\vec{a}_2$  and  $\vec{t}_2 = -\vec{a}_1 + (m+n)\vec{a}_2$  [21]. The unit supercell contains  $N = 4(m^2 + mn + n^2)$  atoms and its periodicity results  $D = a_0/[2 \sin(\theta/2)]$  [12, 15]. Thus, commensurable unit supercells are completely defined by the index  $m$  and  $n$  and those selected to this study appear in Table 1 with their corresponding number of atoms  $N$ , rotation angle between layers  $\theta$  and periodicity  $D$ . For example, the unit supercell for twisted bilayer graphene with the angle  $7.3^\circ$  is shown in Figure 1(b).

**Table 1.** Selected commensurable unit supercells and their corresponding number of constituent atoms ( $N$ ), rotation angle ( $\theta$ ) and periodicity ( $D$ ). The last column shows periodicities experimentally reported.

m	n	N	$\theta$	D (nm)	D Exp. (nm)
2	1	28	$21.8^\circ$	0.65	0.65 Ref. [24]
3	2	76	$13.2^\circ$	1.05	1.06 Ref. [25] 0.95 Ref. [26]
4	3	148	$9.4^\circ$	1.50	1.50 Ref. [27] 1.50 Ref. [28]
5	4	244	$7.3^\circ$	1.91	1.76 Ref. [29] 1.71 Ref. [30]
6	5	364	$6.0^\circ$	2.30	2.20 Ref. [31] 2.40 Ref. [32]

Our DFT calculations were carried out using the SIESTA *ab initio* package [33] which employ norm-conserving pseudopotentials and localized atomic orbitals as basis set. Double- $\zeta$  plus polarization functions were used under the local density approximation [34]. All structures were fully relaxed until the atomic forces are smaller

than 0.02 eV/Å. We consider supercells with periodic boundary conditions for the plane layers, while in the perpendicular direction to the layers plane the separation between slabs is fixed to 14 Å. The Brillouin zone sampling was performed using a Monkhorst-Pack mesh of  $10 \times 10 \times 1$ .

The images were obtained using the code *STM* 1.0.1 (included in the SIESTA package). This code uses the wavefunctions generated by SIESTA and computed on a reference plane and extrapolates the value of these wavefunctions into vacuum. Such reference plane must be sufficiently close to the surface so that the charge density is large and well described. The STM data is generated under the Tersoff-Hamann theory [9], while data visualization was possible using the WSxM 5.0 freeware [35]. Gaussian smooth was performed to obtain the final STM image.

### 3. Results

Electronic properties and constant height mode STM images were calculated for the five commensurable supercells presented in Table 1. Figure 2 shows band structure and total density of states (DOS) for three of these twisted bilayer graphene. Clearly, a decrease of the rotation angle  $\theta$  diminishes the energy difference between the VHS near the Fermi Level. This effect was reported in previous works [7, 21, 36] and has its origin in the renormalization of Dirac electrons velocities, which is observed in the band structures as a decreasing in the slope of the Dirac cone. Additionally the VHSs show the well known asymmetry between electrons and holes, which is observed as a difference in the height of the VHSs. These theoretical predictions have been recently corroborated by STM/STS experimental measurements on twisted graphene layers with  $\theta = 1.79^\circ$  [7] and ensure us that our calculations reproduce the main electronic characteristics of the twisted bilayer graphene.

As the occupied states contributing to the STM image are in the energy window  $[E_{Fermi} - e|V_{bias}|, E_{Fermi}]$  [9, 10], the STM image bias voltage dependence was studied by considering several values in the range  $0.05 \text{ V} < V_{bias} < 3.0 \text{ V}$ . As example, Figure 3 shows calculated STM images and their corresponding line profiles for the case  $V_{bias} = 1.0 \text{ V}$  and the tip-to-surface distance  $d_{TS} = 1.0 \text{ Å}$ . These calculated STM images show bright zones indicating tunnel current maxima, which form triangular structures with periodicities much larger than the graphite lattice constant. These *superlattice constants* correspond to the periodicities  $D$  shown in Table 1. Another important result derived from these calculations is that the brilliant zones are over the AA stacked regions in accordance with the proposal of other authors: Rong and Kuiper [13] and Campanera et al. [19], who based their conclusions in DOS calculations for different stacking sequence of graphite [14]; and Trambly de Laissardiere et al. [21], who combined tight-binding with ab-initio calculations to study the LDOS on twisted bilayer graphene.

Line profiles were performed along the segment indicated in each STM image of Figure 3. Although the calculated images correspond to constant height mode, the line

profiles might be compared with those experimentally obtained in constant current mode assuming that depressions in the charge density lead to proportional approximations of the tip-to-the-surface in order to keep the tunnel current constant. So, our results show two important features revealed also during the STM experiments: a roughness presenting the graphite periodicity and a large oscillation amplitude presenting the superlattice periodicity [12, 13, 15]. For the first case, the roughness reflects the electronic charge accumulation at the atomic sites, which is detected by STM tip. For the second case, the oscillation amplitude is much more larger than the roughness due to the atomic sites and it has been named “giant” or “superlattice corrugation” [15]. Clearly our calculations suggests that the physical origin of the *superlattice corrugation* is mainly an electronic effect and consequently the wide gamma of alternative explanations (see [15] and references therein) seems to be less important at least for STM images of BLG. Also we found, coinciding with the experimental observations on graphite surfaces [13, 15], that bias voltage has a strong influence in the *Superlattice Corrugation Amplitude* (SCA). Figure 4 shows SCA obtained from calculated STM for the rotation angles under study and with different bias voltages. The SCA corresponding to  $\theta = 21.8^\circ$  is the smaller one and presents a current maximum at  $\approx 1.0$  V. Such SCA maximum seems to be a consequence of the DOS which, in the case  $\theta = 21.8^\circ$ , shows the first VHS at  $\approx -1.0$  V. Of course the main contribution to this VHS comes from the Local Density of States (LDOS) over the AA stacked regions, but the decrease of SCA for  $V_{bias} > 1.0$  V is evidence that from that value other regions start to contribute to the DOS. For lower rotation angles, as i.e.  $9.4^\circ$  and  $7.3^\circ$ , the first VHS occurs closer to the Fermi Energy (see Fig. 2) and its main contribution comes from the AA stacked regions. However when the bias voltage increases over 2.0 V the LDOS from other regions start to contribute equally and SCA starts to diminish. Such behavior for the LDOS was also experimentally revealed by STS on the bright and dark regions of STM data [7, 24].

On the other hand the STM dependence on the tip-to-sample distance ( $d_{TS}$ ) was also studied by considering different values in the range  $1.0 \text{ \AA} < d_{TS} < 2.0 \text{ \AA}$ . Thus, the present STM image generation methodology shows that the tip-to-surface distance has no consequence in the calculated STM images and current intensity maxima remain over the regions with large concentration of  $\alpha$ -sites (AA regions). This result indicates that the STM image generation methodology is well defined in the  $d_{TS}$  range considered, but does not give definitive conclusions about tip-to-sample distance dependences as those theoretically predicted [20] and experimentally observed [6] for trilayer graphene case.

#### 4. Conclusions

From ab-initio methods we have calculated constant height mode STM images for twisted graphene bilayer presenting five commensurable rotation angles. The calculated images show superstructures as those revealed during STM characterization of graphite surface and reproduce their main features. In particular the line profiles, obtained from the calculated images, show two important features experimentally observed: a large

oscillation amplitude (giant corrugation) with the periodicity of the superstructures; and a roughness with the graphene lattice periodicity. Thus, these results are showing that the superstructures have a strong electronic origin and, therefore, mechanical tip-sample interaction, or another physical grounds, are not always relevant to explain the phenomena.

Three additional important conclusions derived from this study must be remarked: first, despite the weak interlayer interaction, a relative rotation between them can modify considerably the surface electronic structure; second, results show clearly that, for twisted bilayer graphene, the current intensity maxima appear over *AA* stacked regions; and third, the bias voltage has a strong influence in the *superlattice corrugation* amplitude.

## Acknowledgments

This work was partially supported by Universidad de La Frontera, under Project DI11-0012. J. D. acknowledges FONDECYT postdoctoral program under Grant No. 3110123. We thank Centro de Modelación y Computación Científica (CMCC), Universidad de La Frontera, by computational facilities and programming help. Dr. Marcos Flores is gratefully acknowledged for useful discussions.

## References

- [1] Geim A K and Novoselov K S 2007 Nat. Mat. **6** 183
- [2] Kobayashi Y, Fukui K, Enoki T and Kusakabe K 2006 Phys. Rev. B **73** 125415
- [3] Niimi Y, Matsui T, Kambara H, Tagami K, Tsukada M and Fukuyama H 2006 Phys. Rev. B **73** 085421
- [4] Kuwabara M, Clark D R and Smith D A 1990 Appl. Phys. Lett. **56** 2396
- [5] Loginova E, Nie S, Thürmer K, Bartelt N and McCarty K 2009 Phys. Rev. B **80** 085430
- [6] Miller D L, Kubista K D, Rutter G M, Ruan M, de Heer W A, First P N and Stroscio 2010 J Phys. Rev. B **81** 125427
- [7] Li G, Luican A, Lopes dos Santos J M B, Castro Neto A H, Reina A, Kong J and Andrei E Y 2010 Nat. Phys. **6** 109
- [8] Tománek D and Louie S G 1988 Phys. Rev. B **37** 8327
- [9] Tersoff J and Hamman D R 1983 Phys. Rev. Lett. **50** 1998
- [10] Selloni A, Carnevali P, Tosatti E and Chen C D 1985 Phys. Rev. B **31** 2602
- [11] Cisternas E, Stavale F, Flores M, Achete C A and Vargas P 2009 Phys. Rev. B **79** 205431
- [12] Xhie J, Sattler K, Ge M and Venkateswaran N 1993 Phys. Rev. B **47** 15835
- [13] Rong Z Y and Kuiper P 1993 Phys. Rev. B **48** 17427
- [14] Charlier J-C, Michenaud J-P and Gonze X 1992 Phys. Rev. B **46** 4531
- [15] Pong W -T and Durkan C 2005 J. Phys. D: Appl. Phys. **38** R329
- [16] Zeinalipour-Yazdi C D and Pullman D P 2008 Chem. Phys. **348** 233
- [17] Khara G S and Choi J 2009 J. Phys.: Cond. Matter **21** 195402
- [18] Wong H S, Durkan C and Chandrasekhar N 2009 ACS Nano **11** 3455
- [19] Campanera J M, Savini G, Suarez-Martinez I and Heggie M I 2007 Phys. Rev. B **75** 235449
- [20] Cisternas E, Flores M and Vargas P 2008 Phys. Rev. B **78** 125406
- [21] Trambly de Laissardière G, Mayou D and Magaud L 2010 Nano Lett. **10** 804
- [22] Kolmogorov A N and Crespi V H 2005 Phys. Rev. B **71** 235415

- [23] Shallcross S, Sharma S, Kandelaki E and Pankratov O A 2010 Phys. Rev. B **81** 165105
- [24] Luican A, Li G, Reina A, Kong J, Nair R R, Novoselov K S, Geim A K and Andrei E Y 2011 Phys. Rev. Lett. **106** 126802
- [25] Nysten B, Roux J -C, Flandrois S, Daulan C and Saadaoui H 1993 Phys. Rev. B **48** 12527
- [26] Moreno López J C, Passeggi Jr M C G, Ferrón J 2008 Surf. Sci. **602** 671
- [27] Elings V and Wudl F 1988 J. Vac. Sci. Technol. A **6** 412
- [28] Song I K, Kitchin J R and Barteau M A 2002 Proc. Natl. Acad. Sci. **99** 6471
- [29] Albrecht T R, Mizes H A, Nogami J, Park S and Quate C F 1988 Appl. Phys. Lett. **52** 120
- [30] Miyake K, Akutsu K, Yamada T, Hata K, Morita R, Yamashita M and Shigekawa H 1998 Ultramicroscopy **73** 185
- [31] Tanii T, Hara K, Ishibashi K, Ohta K and Ohdomari I 2000 Appl. Surf. Sci. **162** 662
- [32] Yang Y, Bromm Ch, Geyer U and von Minnigerode G 1992 Ann. Phys. **1** 3
- [33] Soler J M, Artacho E, Gale J D, Garcia A, Junquera J, Ordejón P and Sánchez- Portal J D 2002 J. Phys. Condens. Matter. **14** 2745
- [34] Ceperley D M and Alder B J 1980 Phys. Rev. Lett. **45** 566
- [35] Horcas I, Fernandez R, Gomez-Rodriguez J M, Colchero J, Gomez-Herrero J, and Baro A M 2007 Rev. Sci. Instr. **78** 013705
- [36] Suárez Morell E, Correa J D, Vargas P Pacheco M and Barticevic Z 2010 Phys. Rev. B. **82** 121407



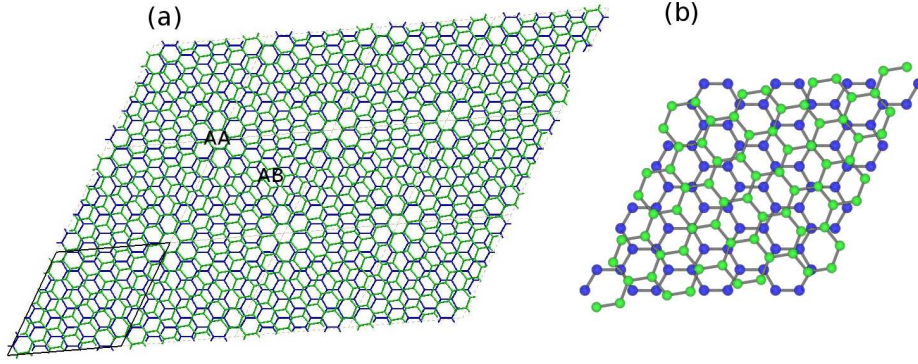


**Figure 1.** (a) Scheme view of twisted bilayer graphene for  $7.3^\circ$  as rotation angle. (b) Magnification of the unit supercell which expands the superstructure. Green sticks are

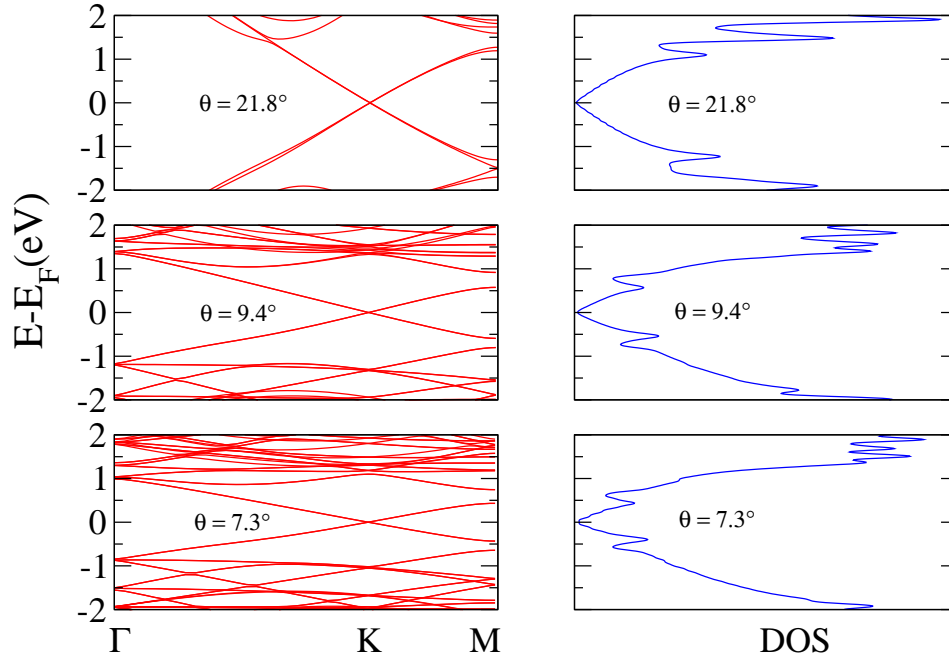


**Figure 2.** Bands structure and total density of states for different twisted bilayer of graphene. Left panels show the bands structures and right panels show the total density of states.



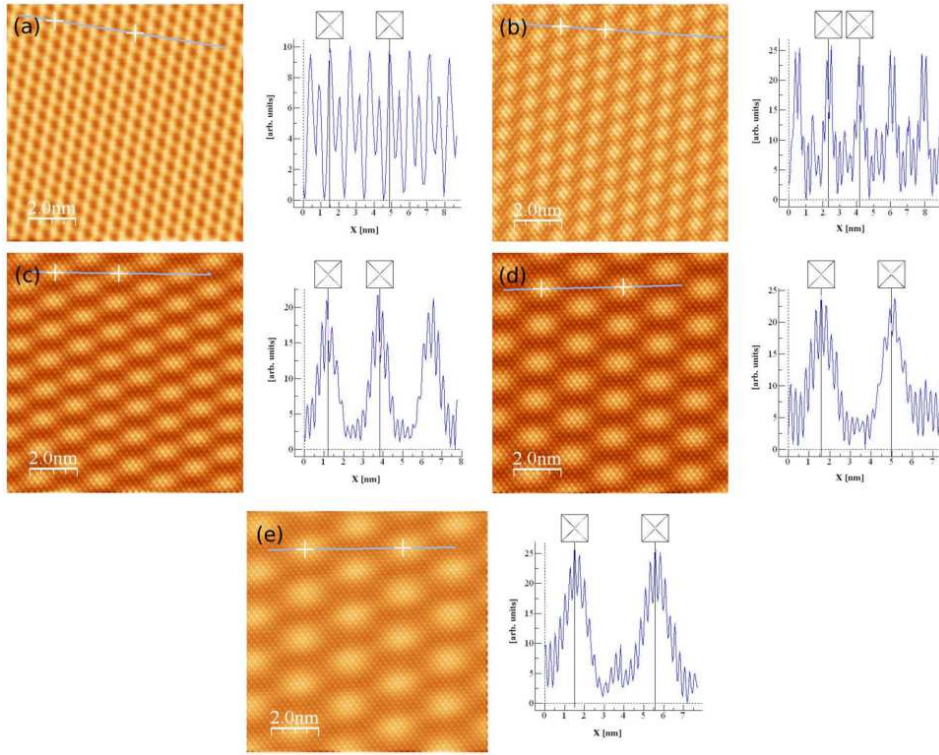


**Figure 3.** Constant height mode STM images calculated for the five commensurable unit supercells presented in Table 1. The line profiles (along the line indicated on the corresponding STM image) appears at right of each one.

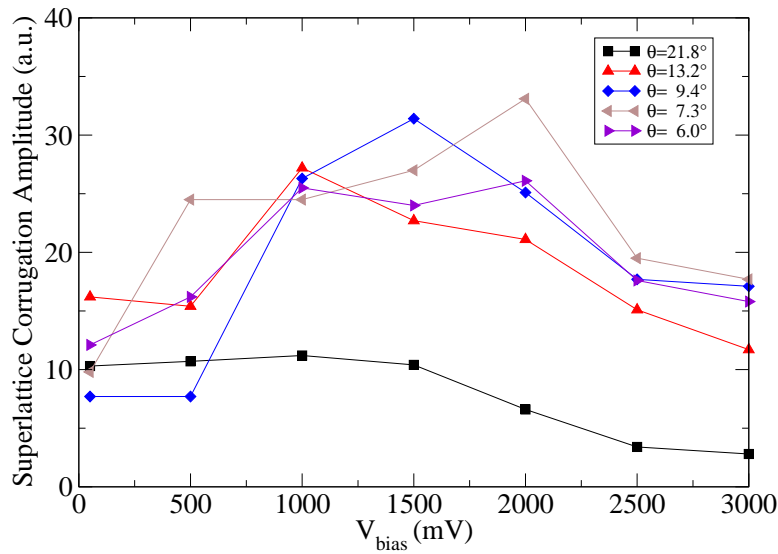


**Figure 4.** Superlattice Corrugation Amplitude on calculated STM images as a function of bias voltages. The rotation angles for the twisted BLG are indicated in the figure.